Original Article

25-hydroxyvitamin D-1α-hydroxylase (CYP27B1) induces ectopic calcification

Yilimulati Yimamu,[1,†] Ayako Ohtani,[1,†] Yuichiro Takei,[2] Airi Furuichi,[1] Yuki Kamei,[1] Hisami Yamanaka-Okumura,[1] Hirokazu Ohminami,[1] Masashi Masuda,[1] Makoto Miyazaki,[3] Hironori Yamamoto,[4] and Yutaka Taketani[1,*]

[1]Department of Clinical Nutrition and Food Management, Tokushima University Graduate School of Medical Nutrition, 3-18-15 Kuramoto-cho, Tokushima 770-8503, Japan
[2]Faculty of Nutrition, University of Kochi, 2751-1, Ike, Kochi 781-8515, Japan
[3]Division of Renal Diseases, Department of Medicine, University of Colorado Anschutz Medical Campus, 13001 East 17th Place, Aurora, CO 80045, USA
[4]Department of Health and Nutrition, Faculty of Human Life, Jin-ai University, 3-1-1 Ohde-cho, Echizen, Fukui 915-8568, Japan

(Received 5 February, 2022; Accepted 15 February, 2022; Released online in J-STAGE as advance publication 4 June, 2022)

Vascular calcification is an important pathogenesis related to cardiovascular disease and high mortality rate in chronic kidney disease (CKD) patients. It has been well-known that hyperphosphatemia induces osteochondrogenic transition of vascular smooth muscle cells (VSMCs) resulting ectopic calcification in aortic media, cardiac valve, and kidney. However, the detailed mechanism of the ectopic calcification has been not clarified yet. Here, we found that the co-localization of CYP27B1 with the calcified lesions of aorta and arteries in kidney of klotho mutant (*kl/kl*) mice, and then investigated the role of CYP27B1 in the mineralization of the VSMCs. Under high phosphate condition, overexpression of CYP27B1 induced calcification and osteocalcin mRNA expression in the VSMCs. Inversely, siRNA-*CYP27B1* inhibited high phosphate-induced calcification of the VSMCs. We also found that the accumulated CYP27B1 protein was glycosylated in the kidney of *kl/kl* mice. Therefore, overexpression of CYP27B1-N310A and CYP27B1-T439A, which are a mutation for *N*-linked glycosylation site (N310A) and a mutation for *O*-linked glycosylation site (T439A) in CYP27B1, decreased calcium deposition and expression of RUNX2 induced by high phosphate medium in VSMCs compared with wild-type CYP27B1. These results suggest that extra-renal expression of glycosylated CYP27B1 would be required for ectopic calcification of VSMCs under hyperphosphatemia.

***Key Words*: hyperphosphatemia, medial calcification, arteriosclerosis, chronic kidney disease, dialysis, bone and mineral disease**

Hyperphosphatemia is a common electrolyte disorder in chronic kidney disease (CKD), and a leading cause of CKD-mineral and bone disorder (CKD-MBD) that is characterized laboratory abnormalities, bone abnormality, and vascular calcification.[1] CKD-MBD is closely related to cardiovascular morbidity and mortality, and all cause mortality in CKD patients.[1,2] CKD patients have highly prevalence of Mönckeberg type arteriosclerosis as well as atherosclerosis.[3] Mönckeberg type arteriosclerosis is a pathognomonic vascular pathology in CKD patients, especially with chronic dialysis, which is characterized by medial arterial calcification, so-called vascular calcification.[3,4] Vascular calcification is an actively regulated process in which vascular smooth muscle cells (VSMCs) acquire osteoblast-like phenotype rather than passive mineral precipitation.[4–6] Until now, many researchers have tried to clarify the mechanism of vascular calcification by hyperphosphatemia. Hyperphosphatemia is the most well-known inducer of vascular calcification, and induces the expression of RUNX2, a master regulator of osteoblast differentiation in VSMCs instead of MyoD, a master regulator of muscular cells, and normally expressed in VSMCs.[7] This is well-known theory that elevation of extracellular inorganic phosphate (Pi) levels induced osteochondrogenic trans-differentiation of vascular smooth muscle cells, or osteochondrogenic differentiation of mesenchymal stem cells in arterial wall. So far type III sodium dependent phosphate transporter (SLC20A1 and SLC20A2) and P-linked glucose-6-phosphate antiporter/Pi exchanger (SLC37A2) have been identified as key molecules related to calcification of vascular smooth muscle cells induced by hyperphosphatemia under CKD.[7,8] However, the detailed pathogenetic mechanism remains unknown.

Renal Pi reabsorption is the rate limiting step in systemic Pi homeostasis, and is tightly regulated by parathyroid hormone (PTH) and fibroblast growth factor 23 (FGF23).[9] FGF23 binds to FGF receptors with klotho which is a co-receptor for FGF23.[10] Therefore, both klotho mutant (*kl/kl*) and FGF23 knock-out mice exhibit similar premature aging-like phenotypes such as a short lifespan, infertility, decreased bone mineral density, and ectopic calcification.[10,11] These mice also show high circulating levels of Pi and 1α,25-dihydroxyvitamin D [1α,25$(OH)_2$D] and develop arterial medial calcification. 1α,25$(OH)_2$D is another Pi regulating factor that can increase both intestinal Pi absorption and renal Pi reabsorption. 1α,25$(OH)_2$D is mainly produced from 25-hydroxyvitamin D in the renal proximal tubule by 25-hydroxyvitamin D-1α-hydroxylase (CYP27B1).[10] The expression of CYP27B1 is tightly regulated by PTH positively and FGF23 negatively.[12] CYP27B1 is mainly located in the kidney but it can be found in various extra-renal tissues including VSMCs, myocardium, lung, colon, and testis.[13,14] Recently, Torremade *et al.*[15] reported that CKD induced expression of CYP27B1 in vascular smooth muscle cells and the extra-renal expression of CYP27B1 mediated vascular calcification. Klotho expresses in renal tubule and the renal klotho expression decreased in CKD patients and model animals such as CKD and ageing.[16,17] The *kl/kl* mice as well as CKD model animals exhibits ectopic calcification, suggesting that overexpression of CYP27B1 must be observed and related to pathogenesis of *kl/kl* mice.

Here, we report that CYP27B1 expressed in ectopic calficied tissues such as artery and kidney in *kl/kl* mice, and the expressed CYP27B1 would be modified by glycosylation. In addition, we investigated the role of glycosylation in the CYP27B1-mediated calcification in VSMCs.

[†]YY and AO equally contributed to this work.
*To whom correspondence should be addressed.
E-mail: taketani@tokushima-u.ac.jp

doi: 10.3164/jcbn.22-16

Materials and Methods

Experimental animals. All animals were maintained climate-controlled room (22 ± 2°C) with 12 h:12 h dark-light cycles under pathogen-free conditions and handled in accordance with the Guidelines for Animal experimentation of the Tokushima University. The protocol of all animal experiments were approved by Animal experiment committee of the Tokushima University.

Heterozygous klotho mutant (*kl*/+) mice were purchased from Japan CLEA, Inc (Osaka, Japan). Homozygous klotho mutant (*kl/kl*) mice were generated by crossing *kl*/+ mice and wild type (WT) mice. Mice were weaned at 3 weeks of age and given free access to water and standard mouse chow (Oriental Yeast, Osaka, Japan) under pathogen-free condition. WT and *kl/kl* mice were sacrificed at 3- and 6-week-old. For biochemical analysis of plasma, blood was collected with heparin by puncture of inferior vena cava. The plasma levels of Ca and Pi were determined by Calcium-E test (Wako Pure Chemical Industries, Ltd., Osaka, Japan) and Phospha-C test (Wako), respectively.

Immunohistochemical analysis. Harvested mouse tissues were fixed with 4% paraformaldehide in phosphate buffered saline (PBS), and then dehydrated in ascending ethanol series, embedded in paraffin and sliced at 2 μm thickness. After consuming endogenous peroxidaze with 3% H_2O_2 for 10 min, slides were pre-incubated with 1% bovine serum albumin (BSA)/PBS to block nonspecific reactions and then incubated with polyclonal goat anti-CYP27B1 antibody (Santa Cruz, Dallas, TX, 1:200 dilution) or rabbit anti-NaPi-IIa antibody (1:1,000 dilution) for overnight at 4°C.[18] Biotin-conjugated rabbit anti-goat IgG or goat anti-rabbit IgG were used as the second antibody followed by a treatment with peroxidase-streptavidin complex [Histofine SAB-PO (goat) kit; Nichirei, Tokyo, Japan]. The sections were stained with a solution containing 0.03% 3'3-diaminobenzidine tetrahydrochloride (DAB; Thermo Fisher Scientific K.K., Kanagawa, Japan), 0.001% H_2O_2 (Wako), 10 mM Imidazole (Wako) and 50 mM Trizma hydrochloride (Sigma-Aldrich Japan, Tokyo, Japan). Mayer's Hematoxylin Solution (Wako) was used for nuclear counterstaining. The specificity of polyclonal goat anti-CYP27B1 antibody was confirmed by peptide neutralization outlined above and decalcification test as described below. Furthermore, no specific signal is obtained with normal goat IgG (sc-2028, Santa Cruz, 1:400 dilution).

Decalcification was performed to make clear whether or not CYP27B1 protein accumulated in hydroxyapatite. Deparaffinized and dehydrated tissue sections were decalcified by incubating in 0.6 N hydrochloric acid (HCl) for 24 h at room temperature. Von Kossa staining was used to evaluate decalcification treatment. The other series sections underwent same decalcification process were used for immunohistochemistory.

Von Kossa stain was performed as previously described.[19] In brief, the tissue sections were treat with 5% silver nitrate solution under ultraviolet light for 1 h. The sections were then washed with distilled water and immersed in 5% sodium thiosulfate solution. Sections were also counterstained with hematoxylin-eosin (HE).

Western blot analysis. Isolated tissue was homogenized in lysis buffer [1% Triton X-100, 50 mM Trizma hydrochloric acid (Tris-HCl), 150 mM NaCl, 5 mM EDTA] and centrifuged at 12,000 rpm for 10 min after standing on ice for 10 min. Equal protein roading was verified by Bradford assay using the Bio-Rad Protein Assay (Bio-Rad Laboratories, Inc., Hercules, CA). Supernatants were incubated with 2× sodium dodecyl sulfate (SDS) sample buffer, separated on 12% SDS-polyacrylamide gels, and electroblotted onto polyvinylidene difluoride membranes (Immobilon-P; Millipore Corp., Bedford, MA). Membranes were blocked for 1 h at room temperature with 5% non-fat dried milk in PBS containing 0.05% Tween-20 (PBS-t). The membranes were treated with the primary antibodies used polyclonal goat anti-CYP27B1 (C-12) (1:200 dilution) and anti-β-actin (Sigma-Aldrich Japan, 1:3,000 dilution), the second antibody rabbit anti-goat IgG (H+L) HRP conjugate (Santa Cruz, 1:4,000 dilution) and goat anti-mouse IgG (H+L) HRP conjugate (Invitrogen Life Technologies, Inc., Tokyo, Japan, 1:4,000 dilution) and probed with the primary antibodies for overnight at 4°C and washed three times with PBS-t. The secondary antibody was added for 1 h at room temperature. Signals were detected using the enhanced chemiluminescense (ECL) Plus system (GE Healthcare Japan, Tokyo, Japan) and BioMax MR Film (Kodak Japan Ltd., Tokyo, Japan). The specificity of polyclonal goat anti-CYP27B1 antibody was confirmed by peptide neutralization. Polyclonal goat anti-CYP27B1 antibody was incubated for 2 h at room temperature with a 5-fold excess (weight) of CYP27B1 peptide antigen (sc-49642 P; Santa Cruz) in each block buffer before being used.

Periodic acid-schiff (PAS) stain was also carried out to detect glycosylation of proteins as previous report.[20]

Quantitative real-time RT-PCR analysis. Total RNA was isolated from tissues or cultured cells using TRI reagent (Sigma-Aldrich Japan). First strand cDNA was synthesized from 1 μg of total RNA using a first-strand cDNA synthesis kit (Invitrogen Life Technologies, Inc.) with oligo-dT primer. After cDNA synthesis, real-time PCR was performed in 10 μl mixture contained forward primer, reverse primer and SYBR Green PCR master mix using an Applied Biosystems StepOne Plus q-PCR instrument. The quantification of given genes was expressed as the mRNA levels normalized to a ribosomal housekeeping gene (18S) using the comparative Ct method. For real-time PCR amplification, the primer sequences are shown in Table 1.

Cell culture. Rat aortic smooth muscle cell line (A-10 cells) and murine aortic smooth muscle cell line (MOVAS-1 cells, CRL2797; ATCC, Manassas, VA), were maintained in Dulbecco's modified Eagle's medium (DMEM; Sigma-Aldrich Japan) containing 10% fetal bovine serum (FBS; Sigma-Aldrich Japan), 100 IU/ml penicillin and 100 μg/ml streptomycin (Sigma-Aldrich Japan). A-10 cells were cultured at 37°C in humidified atomosphere of 5% CO_2 and 95% air. For Pi-induced calcification, the cells were seeded at 25,000 cells/cm^2 on collagen-coated plates. Then, the cells were incubated with control (CP) medium

Table 1. Oligonucleotide primers

Gene name	Sense primer	Anti-sense primer
For real-time PCR analysis		
Murine Cyp27b1	5'-ATGGTGAAGAATGGCAGAGG-3'	5'-TAGTCGTCGCACAAGGTCAC-3'
Murine Runx2	5'-TGCACCTACCAGCCTCACCATAC-3'	5'-GACAGCGACTTCATTCGACTTCC-3'
Murine 18S RNA	5'-ACGGAAGGGCACCACCAGGA-3'	5'-CACCACCACCCACGGAATCG-3'
For site-directed mutagenesis		
CYP27B1-N310A	5'-GTCCATCCTGGGAGCTGTGACAGAGTTGC-3'	5'-GCAACTCTGTCACAGCTCCCAGGATGGAC-3'
CYP27B1-T439A	5'-GGGGAGGGTCCCGCCCCCCACCCATTT-3'	5'-AAATGGGTGGGGGGCGGGACCCTCCCC-3'

doi: 10.3164/jcbn.22-16

(DMEM containing 10% FBS and 0.9 mM Pi), or high Pi (HP) medium (DMEM containing 10%FBS and either 4.9 mM Pi for A-10 cells or 4 mM for MOVAS-1 cells) for 4 days. Both medium were changed every 2 days.

Alizarin red S staining. Calcium depositions of the cultures were visualized by Alizarin red S staining. Cells were fixed with PFA/PBS for 10 min. These cells were washed in PBS and then exposed to 1% Alizarin red S (Wako) for 10 min. Alizarin red S was extracted with 10% Cetylpyridinium chloride, and the absorbance at 415 nm was determined by conventional spectrophotometer.

Establishment of stable cell lines, siRNA, and transfection. Human CYP27B1 cDNA was purchased from Open Biosystems and cloned into a pLenti-CMV-Hygro vector (Addgene) via Gateway cloning technique. Substitution of aspargine or threonine to alanine to remove *N*- or *O*-linked glycosylation site (N310A or T439A) from wild-type CYP27B1 expression vector was performed using QuickChange site-directed mutagenesis kit (Agilent Technologies Japan, Tokyo, Japan) with specific primers (Table 1) as previously described method.[21] MOVAS-1 cells were infected lentivirus containing either wild-type *CYP27B1* (CYP27B1-WT) or mutated *CYP27B1* (CYP27B1-N310A or CYP27B1-T439A). Colonies were selected by treatment with 200 μg/ml hygromycin B for 7 days and established as stable expression cell lines. To surpress the expression of CYP27B1, *CYP27B1* siRNA oligonucleotides (RSS300312, RSS300313, and RSS300314) or Stealth RNAi Negative Control Duplexes as a control were purchased from Thermo Fisher Scientific. These siRNA oligonucleotides were transfected to A-10 cells with lipofectamine 3000 (Thermo Fisher Scientific), according to the manufacture's instruction.

Statistical analysis. Data were collected from more than 2 independent experiments, and were expressed as means ± SE. Statistical analysis was carried out using one-way ANOVA with Bonferroni's procedure as post-hoc analysis. All data analysis was performed using GraphPad Prism 5 software (GraphPad Software, San Diego, CA). $P<0.05$ was considered to indicate statistically significance.

Results

Expression of CYP27B1 in *kl/kl* mouse kidney. As same as previous report,[22] 3-week-old *kl/kl* mice showed hyperphosphatemia and hypercalcemia. Plasma phosphate levels showed further increase in 6-week-old *kl/kl* mice compared with 3-week-old *kl/kl* mice, as well as calcium-phosphate product levels (Table 2). Real-time RT-PCR analysis demonstrated that *CYP27B1* mRNA levels in 6-week-old *kl/kl* mouse kidney were significantly higher compared to those of WT mice (Fig. 1A). Compared the *CYP27B1* mRNA expression between cortex and medulla in *kl/kl* mouse kidney, *CYP27B1* mRNA levels significantly increased in cortex rather than in medulla (Fig. 1B). Western blot analysis also showed higher CYP27B1 protein expression in *kl/kl* mouse kidney cortex. Surprisingly, we found a mobility-shifted CYP27B1 bands in *kl/kl* mouse kidney cortex and medulla compared with WT mouse (Fig. 1C). Immunohistochemical analysis revealed that the localization of CYP27B1 protein was mainly in proximal tubules in *kl/kl* mouse kidney cortex and not detectable in medulla (Fig. 1D).

Co-localization of CYP27B1 and calcified lesion in *kl/kl* mouse tissues. Interestingly, CYP27B1 protein was co-stained in von Kossa staining in arteries of *kl/kl* mouse kidney cortex (Fig. 2A). There was also co-localization of CYP27B1 and NaPi-IIa, which is a marker of proximal tubule, however, proximal tubule did not show ectopic calcification, suggesting that ectopic calcification was mainly observed in arteries. Furthermore, we examined extra-renal tissues which develop ectopic calcification. We also observed co-localization of highly expressed CYP27B1 and calcified lesion in 6-week-old *kl/kl* mouse aorta (Fig. 2B). These data indicate that regional up-regulation of CYP27B1 can occur in ectopic calcified lesions of kidney and aorta.

Ectopic calcification may cause non-specific immunoreaction in the immunohistochemical analysis of CYP27B1. To confirm whether the immunoreaction of CYP27B1 was specific or not, we investigate the effect of decalcification on the immunohistochemical analysis of CYP27B1 in kidney and aorta of 6-week-old *kl/kl* mice. As shown in Fig. 3, CYP27B1 positive lesions on decalcified tissue sections were localized on the same lesion of von Kossa positive lesion of tissue sections without decalcification treatment. Therefore, the CYP27B1 positive staining of ectopic calcified lesions was not non-specific immunoreaction.

CYP27B1 protein expression was up-regulated before ectopic calcification occurred in *kl/kl* mice. As previously reported by Kuro-o *et al.*,[22] 3-week-old *kl/kl* mice did not show calcification despite of hyperphosphatemia, but 6-week-old *kl/kl* mice did. Then, we examined whether CYP27B1 can express prior to apparent calcification of tissue or not by comparing 3-week-old and 6-week-old *kl/kl* mice. 3-week-old *kl/kl* mice did not show ectopic calcification in both kidney and aorta, but 6-week-old *kl/kl* mice showed ectopic calcification (Fig. 4A and B). On the other hand, CYP27B1 expression was obserbed in aorta and kidney of both 3- and 6-week-old *kl/kl* mice (Fig. 4A and B). Therefore, CYP27B1 would be expressed in the ectopic calcification site before the site exhibits apparent calcification.

CYP27B1 can be modified by glycosylation in the calcified lesions of the kidney in *kl/kl* mice. As shown in Fig. 1C, we found a mobility-shifted CYP27B1 bands in *kl/kl* mouse kidney. We hypothesized that the mobility-shifted CYP27B1 would be due to post-translational modification such as phosphorylation and glycosylation. First, we examined whether the gel mobility of CYP27B1 can be changed by dephosphorylation with λPPase. However, the gel mobility of CYP27B1 was unchanged (Fig. 5A). As shown in Fig. 5B, the mobility-shifted band of CYP27B1 was also stained by PAS stain that is used for confirmation of glycosylation. These results suggest that CYP27B1 was modified by glycosylation.

Mutated *N*-linked glycosylation of CYP27B1 inhibited mineralization induced by Pi in VSMCs. To determine the role of abnormal expression and glycosylation of CYP27B1 in the ectopic calcification, we examined whether overexpression of

Table 2. Biochemical data of WT and *kl/kl* mice

Plasma	3-week-old		6-week-old	
	WT	*kl/kl*	WT	*kl/kl*
Pi (mg/dl)	8.8 ± 0.45	11.7 ± 0.40**	8.4 ± 0.45	15.5 ± 0.51$^{\#,\P}$
Ca (mg/dl)	9.6 ± 0.38	11.0 ± 0.36*	9.6 ± 0.25	11.0 ± 0.29$^{\#,\P}$
Ca × Pi (mg^2/dl^2)	84.4 ± 6.7	128 ± 7.7**	80.9 ± 5.0	171 ± 7.9$^{\#\#,\P}$

Plasma was collected at 3-week-old and 6-week-old WT and *kl/kl* mice. Data are expressed as means ± SE ($n = 3$). *$p<0.05$, **$p<0.01$ vs 3-week-old WT, $^{\#}p<0.05$, $^{\#\#}p<0.01$ vs 3-week-old *kl/kl*, $^{\P}p<0.01$ vs 6-week-old WT.

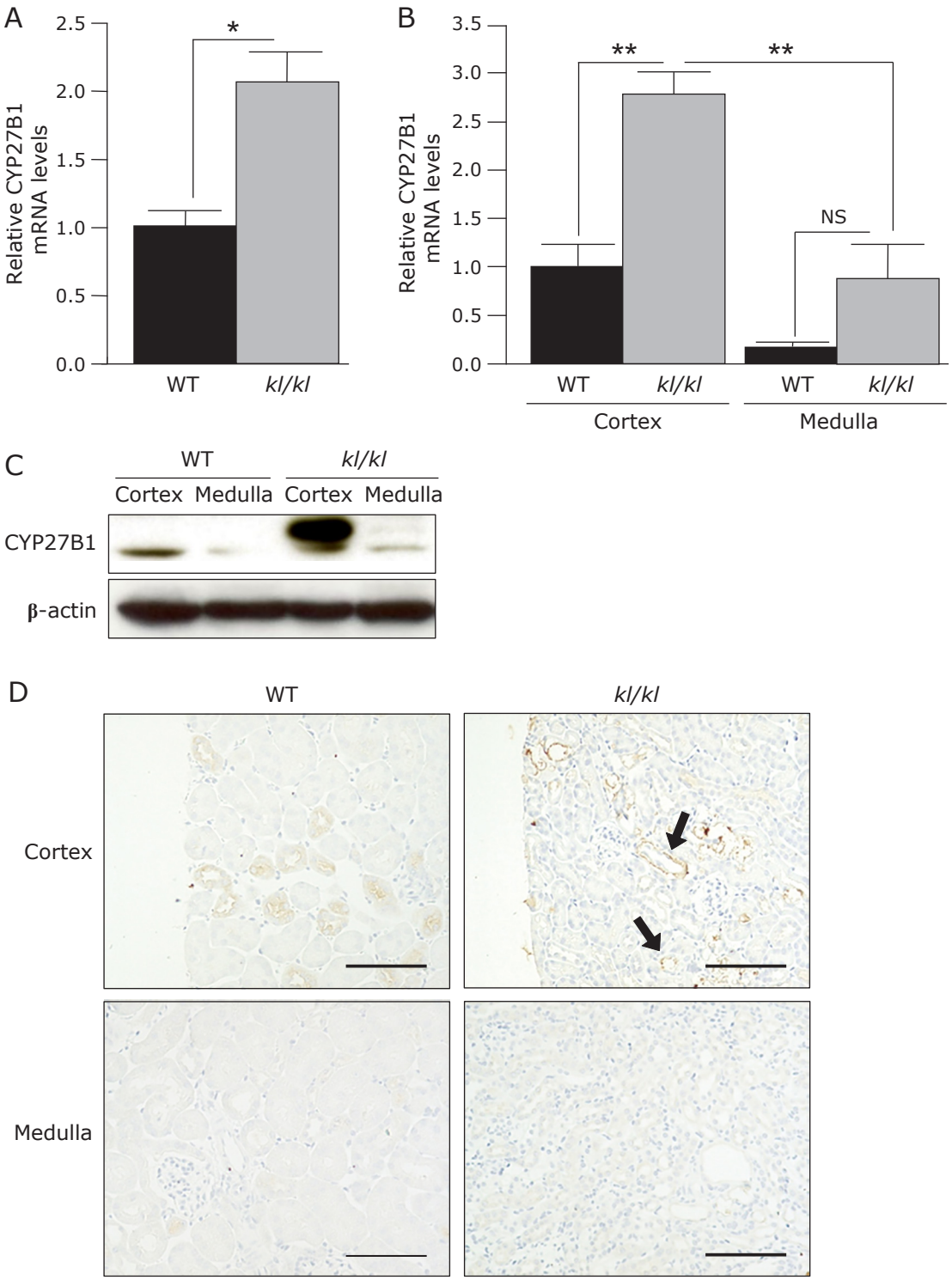

Fig. 1. Overexpression of CYP27B1 and co-localization of CYP27B1 and calcified lesion in *kl/kl* mouse kidney. (A, B) Relative *CYP27B1* mRNA levels of 6-week-old WT and *kl/kl* mouse whole kidney (A), cortex and medulla (B) by real-time RT-PCR. (C) CYP27B1 protein expressions were determined by Western blot analysis using anti CYP27B1 antibody in 6-week-old WT and *kl/kl* mice kidney cortex and medulla. (D) Immunohistocheistry on paraffin sections of kidney shows CYP27B1 protein (arrows) expression in 6-week-old WT and *kl/kl* mice kidney cortex and medulla. CYP27B1 highly expressed in some arteries and tubules of *kl/kl* mouse kidney cortex. (E) Scale bar, 50 μm. Data are representative of at least 3 independent experiments. Quantitative data are reported as means ± SE ($n = 3$, *$p<0.05$, **$p<0.01$).

wild type or mutant CYP27B1 can induce calcification of A-10 cells under high phosphate medium. Alizarin red S stain showed that overexpression of CYP27B1 significantly induced calcification of rat VSMCs in HP medium, not CP medium (Fig. 6A). On the other hand, siCYP27B1 significantly decreased HP medium-induced calcification of A-10 cells (Fig. 6B). MOVAS-1 cells

doi: 10.3164/jcbn.22-16

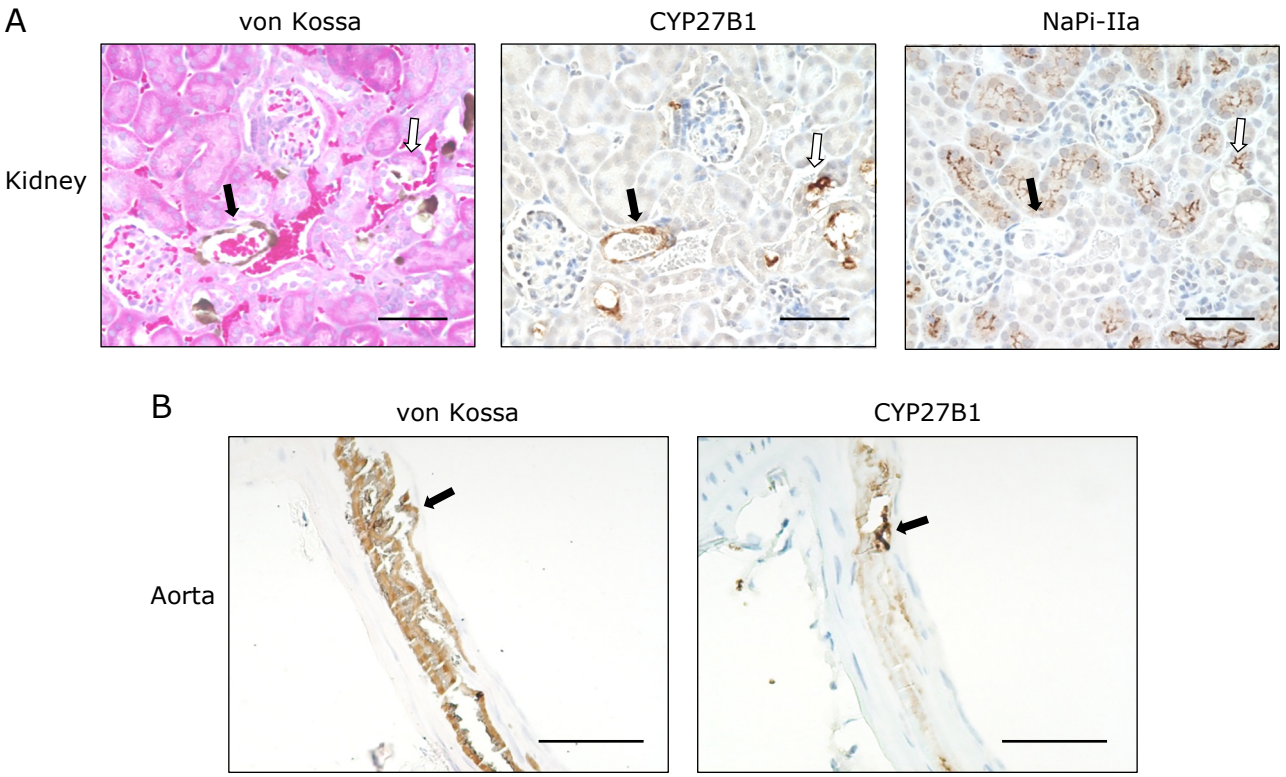

Fig. 2. Co-localization of CYP27B1 and calcified lesion in *kl/kl* mouse various tissues. Co-localization of immunostaining CYP27B1 protein and von Kossa staining calcified lesion were compared using serial sections of 6-week-old *kl/kl* mouse kidney (A) and aorta (B). (A) CYP27B1 positive signals were found in both artery (black arrows) and proximal tubule (white arrows) that confirmed by anti-NaPi-IIa antibody. On the other hand, positive signals in von Kossa staining found in artery of the *kl/kl* mice kidney. (B) CYP27B1 positibe lesion co-localized in von Kossa positive lesion in aorta. Scale bar 50 μm. Data are representative of at least 3 independent experiments.

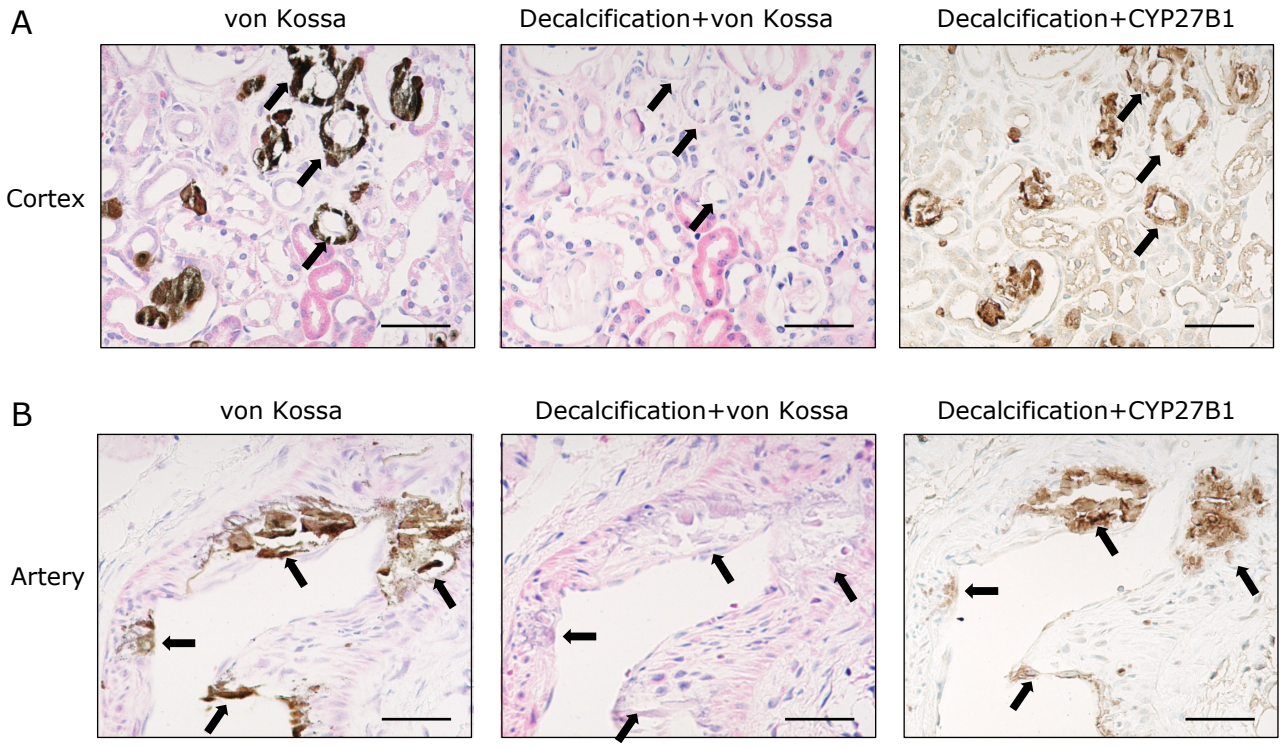

Fig. 3. Ectopic calcification did not affect immunostaining with anti-CYP27B1 antibody. Serial sections from kidney (A) and aorta (B) of 6-week-old *kl/kl* mice were analyzed by von Kossa staining and immunostaining of CYP27B1. Left panel shows calcified lesions on tissue sections without decalcification by von Kossa staining (arrows). Center panels shows no positive stain of von Kossa staining on decalcificated sections (arrows). Right panels shows CYP27B1 positive signals were obserbed in the same location as calcified lesion on decalcificated sections (arrows). Scale bar, 50 μm.

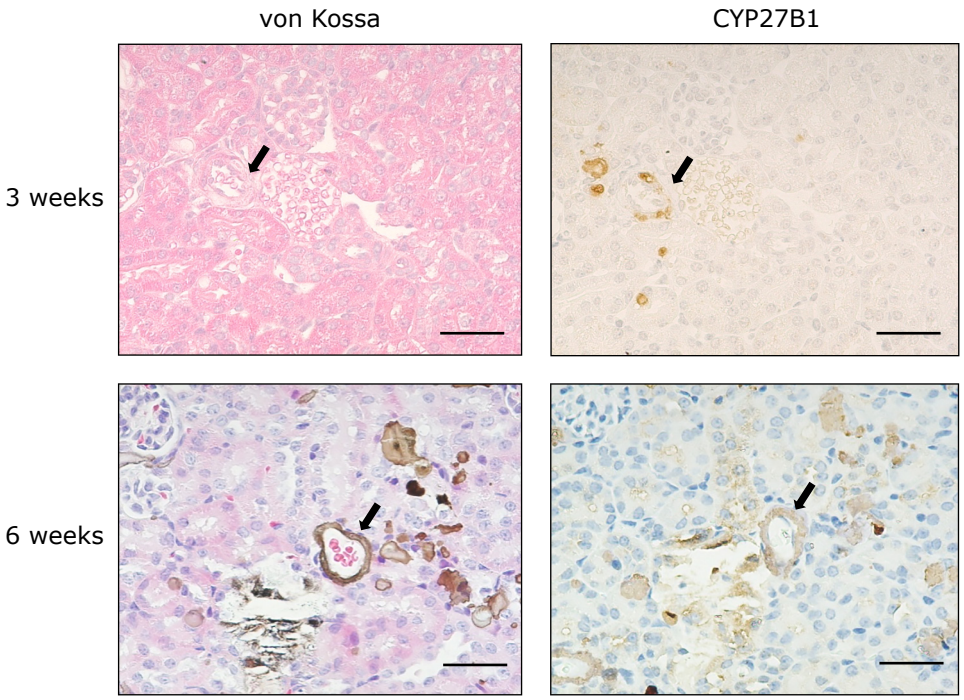

Fig. 4. CYP27B1 was expressed before development of ectopic calcification in 3-week-old *kl/kl* mouse kidney. Von Kossa staining and CYP27B1 immunohistochemistry in 3-week-old (upper panels) and 6-week-old *kl/kl* mouse (lower panels) kidney cortexes. Paraffin sections were stained by von Kossa staining and CYP27B1 immunohistochemistry. Scale bar, 50 μm. Data are representative of at least 3 independent experiments.

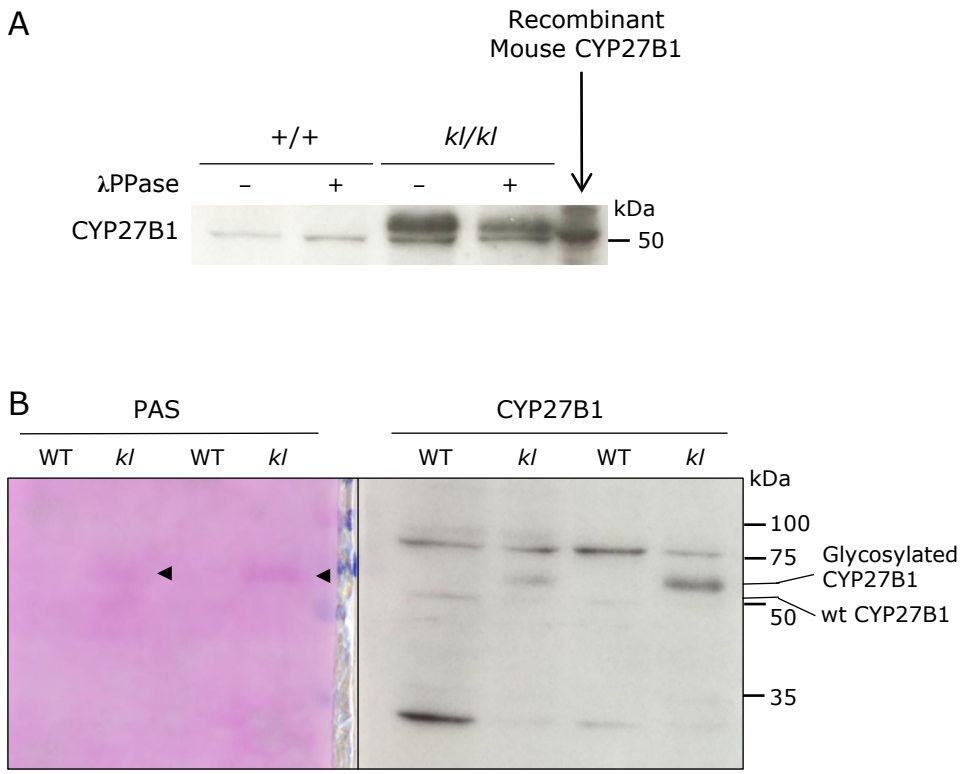

Fig. 5. CYP27B1 protein was modified by glycosylation, not phosphorylation in *kl/kl* mouse kidney. (A) Protein extracts of 6-week-old *kl/kl* mouse kidney were dephosphorylated with or without lambda protein phosphatase (λPPase), then were subjected to Western blot analysis with anti-CYP27B1 antibody. (B) Protein extracts of 6-week-old *kl/kl* mice kidney were blotted to membrane and then were subjected to PAS staining or Western blot analysis with anti-CYP27B1 antibody. Data are representative of at least 3 independent experiments.

doi: 10.3164/jcbn.22-16

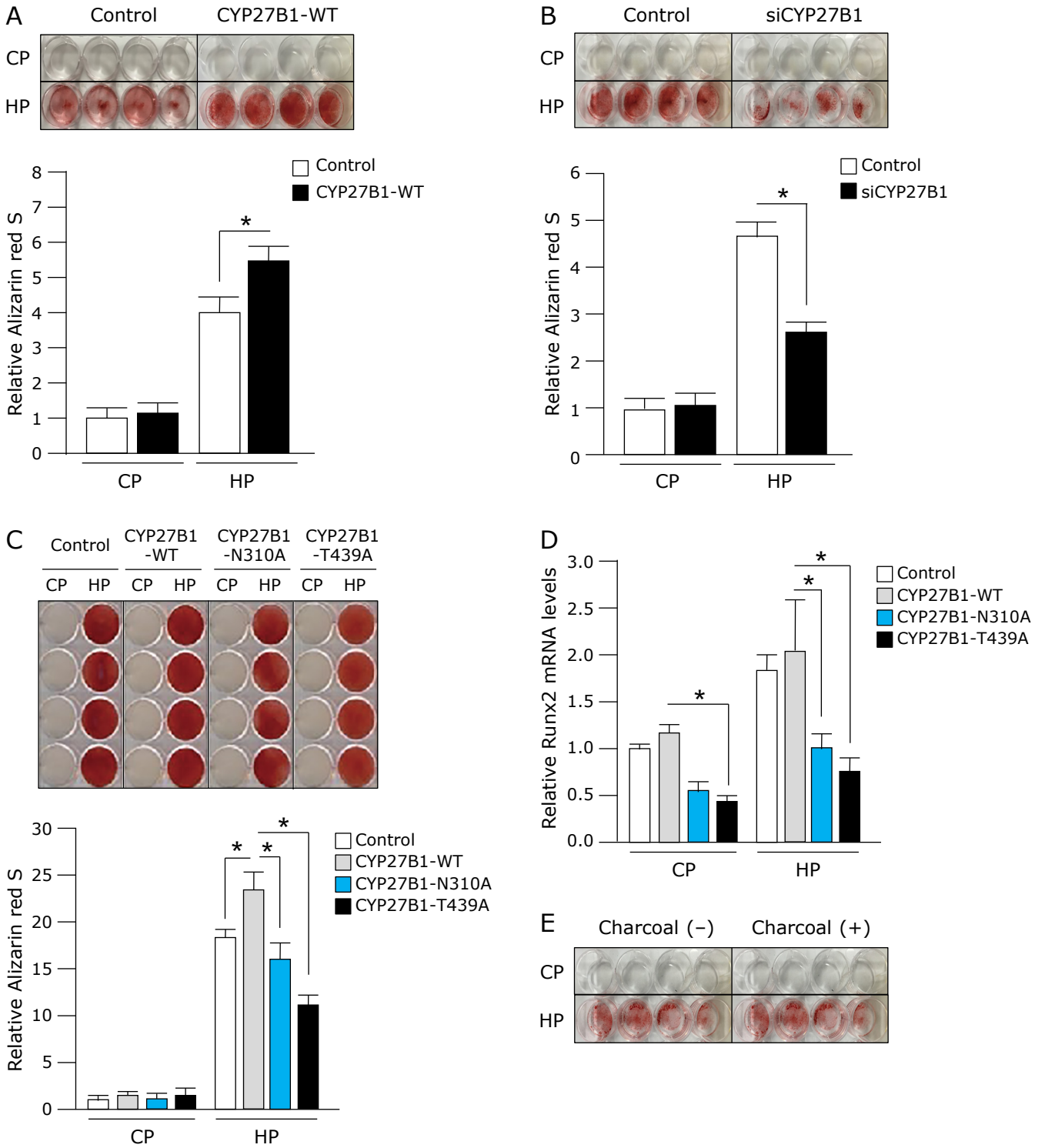

Fig. 6. Overexpression of CYP27B1 plays the key role in ectopic calcification of vascular smooth muscle cells (A-10 cells). (A) A-10 cells were stably transfected with control or wild-type CYP27B1 expression vectors (CYP27B1-WT), then the cells were treated with control medium (CP) or high Pi (HP) medium for 4 days. Calcium depositions were visualized by arizarin red S staining (upper panels) and quantified the extraction of arizarin red S by spectrophotometer (lower graphs). (B) A-10 cells were transfected with control or siRNA oligonucleotides for *CYP27B1* (siCYP27B1), then the cells were treated CP or HP medium, and subjected to stain and quantification as above. (C) MOVAS-1 cells were stably transfected with control or wild-type CYP27B1 (CYP27B1-WT), N310A mutant CYP27B1 (CYP27B1-N310A), T439A mutant CYP27B1 (CYP27B1-T439A) expression vectors, respectively, then the cells were treated CP or HP medium, and subjected to stain and quantification as above. (D) *Runx2* mRNA expression levels were estimated in the MOVAS-1 cells were treated as (C). (E) A-10 cells were transfected with CYP27B1-WT vector, then the cells were treated with high Pi medium containing FBS treated with (charcoal +) or without (charcoal –) charcoal for 4 days, then the cells were stained by arizarin red S. Data are representative of at least 3 independent experiments. Quantitative data are reported as means ± SE ($n = 4$, *$p<0.05$).

expressing mutant CYP27B1 at *N*-linked glycosylation site (N310A) and at *O*-linked glycosylation site (T439A) significantly decreased calcification and *Runx2* mRNA expression compared with CYP27B1-WT expressing A-10 cells (Fig. 6C and D).

We also examined whether the production of $1,25(OH)_2D$ may be important for calcification of A-10 cells. As shown in Fig. 6E, both HP medium with charcoal treated serum or without charcoal induced calcification in CYP27B1-WT expressing A-10 cells. Thus, local production of $1,25(OH)_2D$ would not be necessary for ectopic calcification.

Discussion

Our results show that extra-renal CYP27B1 expression is associated with ectopic calcification of various soft tissues such as kidney and aorta in *kl/kl* mice. This phenomenon is consistent with the previous report that CYP27B1 mediated vascular calcification in CKD model rats.[15] In addition, overexpressed and glycosylated CYP27B1 would play an important role in the calcification of VSMCs.

CYP27B1 is a cytochrome P450 enzyme and located in mitochondria in renal proximal tubular cells to produce $1,25(OH)_2D$.[23] CYP27B1 can also be expressed in several extra-renal cells such as epithelial cells including keratinocytes, placenta, bone cells, immune cells, and endocrine cells.[14] Roles of extra-renal CYP27B1 have been reported in physiology and pathophysiology in various tissues and cells.[14] According to previous reports, CYP27B1 can be physiologically associated with barrier function in epithelial cells.[24] On the other hand, overexpression of CYP27B1 is found in the early stages of malignancy epithelial cells, suggesting that CYP27B1 would be important in physiological and pathphysiological events.[25,26] In addition, we found CYP27B1 was glycosylated in calcificated tissues. To our knowledge, this is the first report that CYP27B1 can be glycosylated. However, it has been known that a number of cytochrome P450 enzymes can be glycosylated.[27,28] The role of glycosylation in cytochrome P450 enzymes has not been clarified yet, but CYP11A1 and CYP19A1 are known as a glycoprotein and their glycosylation may be related with enzyme catalytic activity.[29,30] The present study demonstrated that overexpression of CYP27B1 induced calcification under the charcoal-treated medium that means vitamin D-free medium, suggesting that enzyme activity of CYP27B1 cannot be related to induce ectopic calcification in VSMCs.

Glycosylation of protein affects intracellular targeting, longevity and/or stability of protein. The glycosylated modification of CYP27B1 may be involved in mislocalization of CYP27B1 and cellular stress. *N*-linked glycosylation is generally occurred in endoplasmic reticulum (ER) and the hydrophilic modification can affect the characteristics and quality control of proteins such as protein stability, solubility, membrane orientation and turnover rate.[31] For instance, *N*-linked glycosylation modification can prevent the protein from proteolysis and denaturation.[32] In our study, overexpressed CYP27B1 observed in *kl/kl* mice was glycosylated, suggested that the glycosylation modification might be used to suffer from proteolysis and be involved in over-accumulation of CYP27B1.

On the other hand, accumulation of ectopically expressed protein can induce ER stress that is physiological response to protein quality control, that removes inappropriately produced proteins to protect cellular function.[33] However, excessive ER stress sometimes leads pathophysiological state in the cells. In human hepatoma cells, overexpression of cytochrome P450 (CYP2C9) induced an ER stress due to protein overexpression rather than mono-oxygenase activity of the enzyme.[34] Ectopic overexpression of CYP27B1 may be also involved in the ER stress in ectopic calcified cells. Recent studies have reported that activating PKR-like endoplasmic reticulum kinase (PERK)-activating transcription factor-4 (ATF-4) signaling pathway in response to ER stress signal can promotes calcification of VSMCs.[35–37] Therefore, *N*-linked glycosylation of CYP27B1 may trigger ER stress by impaired localization of intracellular CYP27B1, which finally leads to ectopic calcification. Unfortunately, we cannot clarified the reason why CYP27B1 must be overexpressed and glycosylated to induce ectopic calcification under hyperphosphatemia. In addition, siRNA of *CYP27B1* did not completely inhibit ectopic calcification in VSMCs. The result suggests that other factors including SLC37A2 can also contribute to induce ectopic calcification,[8] while overexpression of CYP27B1 would be important for development of ectopic calcification. To address those questions, further investigation will be required.

In conclusion, our findings reveal that overexpression of glycosylated CYP27B1 can be induced by ectopic calcified tissues in klotho deficient mice, and would contribute to development of ectopic calcification.

Author Contributions

Conceptualization, YY, YTakei, MMasuda, HY, and YTaketani; Methodology, YY, AO, YTakei, MMasuda, and HY; Investigation, YY, AO, YTakei, AF, YK, HY-O, HO, and MMasuda; Resources, YTakei, MMasuda, MMiyazaki, HY, and YTaketani; Data collection and analysis, YY, AO, YTakei, AF, YK, MMasuda, and HY; Writing-original draft preparation, YY, AO, MMasuda, and YTaketani; Writing-review and editing, YTakei, HY-O, HO, MMasuda, MMiyazaki, HY, and YTaketani; Project Administration and supervision, MMasuda, HY, and YTaketani; Funding acquisition, MMasuda, HY, and YTaketani. All authors have read and agreed to the published version of the manuscript.

Acknowledgments

We thank the Support Center for Advanced Medical Sciences, Tokushima University Graduate School of Biomedical Sciences for technical assistance. This work was supported by JSPS KAKENHI grant numbers JP17K19910, JP17H05061, JP20K21761, JP21H03359 (to MMasuda), JP19K11779 (to HYamamoto), JP19K22811 and JP19H04053 (to YTaketani).

Conflict of Interest

No potential conflicts of interest were disclosed. The sponsors had no role in the study design, execution, interpretation of results, or writing of the manuscript.

References

1 Taketani Y, Koiwa F, Yokoyama K. Management of phosphorus load in CKD patients. *Clin Exp Nephrol* 2017; **21 (Suppl 1)**: 27–36.
2 Hamano T. Vitamin D and renal outcome: the fourth outcome of CKD-MBD? Oshima Award Address 2015. *Clin Exp Nephrol* 2018; **22**: 249–256.
3 McCullough PA, Agrawal V, Danielewicz E, Abela GS. Accelerated atherosclerotic calcification and Monckeberg's sclerosis: a continuum of advanced vascular pathology in chronic kidney disease. *Clin J Am Soc Nephrol* 2008; **3**: 1585–1598.
4 Mizobuchi M, Towler D, Slatopolsky E. Vascular calcification: the killer of patients with chronic kidney disease. *J Am Soc Nephrol* 2009; **20**: 1453–1464.
5 Giachelli CM. Vascular calcification mechanisms. *J Am Soc Nephrol* 2004; **15**: 2959–2964.

doi: 10.3164/jcbn.22-16

6 Giachelli CM. Ectopic calcification: gathering hard facts about soft tissue mineralization. *Am J Pathol* 1999; **154**: 671–675.
7 Shanahan CM, Crouthamel MH, Kapustin A, Giachelli CM. Arterial calcification in chronic kidney disease: key roles for calcium and phosphate. *Circ Res* 2011; **109**: 697–711.
8 Tani M, Tanaka S, Oeda C, *et al*. SLC37A2, a phosphorus-related molecule, increases in smooth muscle cells in the calcified aorta. *J Clin Biochem Nutr* 2021; **68**: 23–31.
9 Quarles LD. Skeletal secretion of FGF-23 regulates phosphate and vitamin D metabolism. *Nat Rev Endocrinol* 2012; **8**: 276–286.
10 Shimada T, Kakitani M, Yamazaki Y, *et al*. Targeted ablation of Fgf23 demonstrates an essential physiological role of FGF23 in phosphate and vitamin D metabolism. *J Clin Invest* 2004; **113**: 561–568.
11 Urakawa I, Yamazaki Y, Shimada T, *et al*. Klotho converts canonical FGF receptor into a specific receptor for FGF23. *Nature* 2006; **444**: 770–774.
12 Perwad F, Portale AA. Vitamin D metabolism in the kidney: regulation by phosphorus and fibroblast growth factor 23. *Mol Cell Endocrinol* 2011; **347**: 17–24.
13 Adams JS, Rafison B, Witzel S, *et al*. Regulation of the extrarenal CYP27B1-hydroxylase. *J Steroid Biochem Mol Biol* 2014; **144 Pt A**: 22–27.
14 Bikle DD, Patzek S, Wang Y. Physiologic and pathophysiologic roles of extra renal CYP27b1: case report and review. *Bone Rep* 2018; **8**: 255–267.
15 Torremadé N, Bozic M, Panizo S, *et al*. Vascular calcification induced by chronic kidney disease is mediated by an increase of 1α-hydroxylase expression in vascular smooth muscle cells. *J Bone Miner Res* 2016; **31**: 1865–1876.
16 Hu MC, Kuro-o M, Moe OW. Klotho and kidney disease. *J Nephrol* 2010; **23 (Suppl 16)**: S136–S144.
17 Yoshikawa R, Yamamoto H, Nakahashi O, *et al*. The age-related changes of dietary phosphate responsiveness in plasma 1,25-dihydroxyvitamin D levels and renal Cyp27b1 and Cyp24a1 gene expression is associated with renal α-klotho gene expression in mice. *J Clin Biochem Nutr* 2018; **62**: 68–74.
18 Tani Y, Sato T, Yamanaka-Okumura H, *et al*. Effects of prolonged high phosphorus diet on phosphorus and calcium balance in rats. *J Clin Biochem Nutr* 2007; **40**: 221–228.
19 Fukuda-Tatano S, Yamamoto H, Nakahashi O, *et al*. Regulation of α-klotho expression by dietary phosphate during growth periods. *Calcif Tissue Int* 2019; **104**: 667–678.
20 Lower BH, Kennelly PJ. The membrane-associated protein-serine/threonine kinase from *Sulfolobus solfataricus* is a glycoprotein. *J Bacteriol* 2002; **184**: 2614–2619.
21 Yamada F, Horie D, Nakamura A, *et al*. Role of serine 249 of ezrin in the regulation of sodium-dependent phosphate transporter NaPi-IIa activity in renal proximal tubular cells. *J Med Invest* 2013; **60**: 27–34.
22 Kuro-o M, Matsumura Y, Aizawa H, *et al*. Mutation of the mouse klotho gene leads to a syndrome resembling ageing. *Nature* 1997; **390**: 45–51.
23 Henry HL. Vitamin D hydroxylases. *J Cell Biochem* 1992; **49**: 4–9.
24 Hewison M, Zehnder D, Chakraverty R, Adams JS. Vitamin D and barrier function: a novel role for extra-renal 1α-hydroxylase. *Mol Cell Endocrinol* 2004; **215**: 31–38.
25 Radermacher J, Diesel B, Seifert M, *et al*. Expression analysis of CYP27B1 in tumor biopsies and cell cultures. *Anticancer Res* 2006; **26**: 2683–2686.
26 Tangpricha V, Flanagan JN, Whitlatch LW, *et al*. 25-hydroxyvitaminD-1α-hydroxylase in normal and malignant colon tissue. *Lancet* 2001; **357**: 1673–1674.
27 Lamb DC, Waterman MR. Unusual properties of the cytochrome P450 superfamily. *Philos Trans R Soc Lond B Biol Sci* 2013; **368**: 20120434.
28 Aguiar M, Masse R, Gibbs BF. Regulation of cytochrome P450 by posttranslational modification. *Drug Metab Rev* 2005; **37**: 379–404.
29 Ichikawa Y, Hiwatashi A. The role of the sugar regions of components of the cytochrome P-450-linked mixed-function oxidase (monooxygenase) system of bovine adrenocortical mitochondria. *Biochim Biophys Acta* 1982; **705**: 82–91.
30 Amarneh B, Corbin CJ, Peterson JA, Simpson ER, Graham-Lorence S. Functional domains of human aromatase cytochrome P450 characterized by linear alignment and site-directed mutagenesis. *Mol Endocrinol* 1993; **7**: 1617–1624.
31 Shrimal S, Cherepanova NA, Gilmore R. Cotranslational and posttranslational N-glycosylation of proteins in the endoplasmic reticulum. *Semin Cell Dev Biol* 2015; **41**: 71–78.
32 Cherepanova N, Shrimal S, Gilmore R. N-linked glycosylation and homeostasis of the endoplasmic reticulum. *Curr Opin Cell Biol* 2016; **41**: 57–65.
33 Lindholm D, Korhonen L, Eriksson O, Kõks S. Recent insights into the role of unfolded protein response in ER stress in health and disease. *Front Cell Dev Biol* 2017; **5**: 48.
34 Narjoz C, Marisa L, Imbeaud S, *et al*. Genomic consequences of cytochrome P450 2C9 overexpression in human hepatoma cells. *Chem Res Toxicol* 2009; **22**: 779–787.
35 Masuda M, Ting TC, Levi M, Saunders SJ, Miyazaki-Anzai S, Miyazaki M. Activating transcription factor 4 regulates stearate-induced vascular calcification. *J Lipid Res* 2012; **53**: 1543–1552.
36 Masuda M, Miyazaki-Anzai S, Levi M, Ting TC, Miyazaki M. PERK-eIF2α-ATF4-CHOP signaling contributes to TNFα-induced vascular calcification. *J Am Heart Assoc* 2013; **2**: e000238.
37 Masuda M, Miyazaki-Anzai S, Keenan AL, *et al*. Activating transcription factor-4 promotes mineralization in vascular smooth muscle cells. *JCI Insight* 2016; **1**: e88646.